B.K. Choudhary*, E. Isaac Samuel, D.P. Rao Palaparti, J. Christopher and M.D. Mathew

Unified Tensile Work Hardening Behaviour of Thin Section Plate and Forged Thick Section 9Cr-1Mo Ferritic Steel

Abstract: Detailed investigation has been performed on tensile work hardening behaviour in terms of the variations of instantaneous work hardening rate ($\theta = d\sigma/d\varepsilon_p$, where σ is true stress and ε_p is true plastic strain) with stress and true plastic strain rate ($\dot{\varepsilon}_p$) for temperature range 300–873 K in two different material conditions, (i) normalised and tempered plate and (ii) quenched and tempered tubeplate forging of 9Cr-1Mo ferritic steel. Both plate and tubeplate forging exhibited two-stage work hardening and three different temperature regimes in the variation of θ with σ. The variations of θ with respect to $\dot{\varepsilon}_p$ exhibited unified work hardening in terms of a single master curve independent of temperature and initial microstructure. θ varied linearly with reciprocal of plastic strain rate, i.e. $1/\dot{\varepsilon}_p$, and as a consequence, linear correlation between the rate of change of true stress and true plastic strain rate independent of temperature and microstructure has been obtained.

Keywords: 9Cr-1Mo steel, tubeplate forging, unified tensile work hardening, work hardening rate, plastic strain rate

PACS® (2010). 81.40.-z, 81.40.Jj, 83.50.-v, 81.40.Ef

***Corresponding author: B.K. Choudhary:** Mechanical Metallurgy Division, Indira Gandhi Centre for Atomic Research, Kalpakkam – 603 102, Tamil Nadu, India, E-mail: bkc@igcar.gov.in
E. Isaac Samuel: Mechanical Metallurgy Division, Indira Gandhi Centre for Atomic Research, Kalpakkam – 603 102, Tamil Nadu, India
D.P. Rao Palaparti: Mechanical Metallurgy Division, Indira Gandhi Centre for Atomic Research, Kalpakkam – 603 102, Tamil Nadu, India
J. Christopher: Mechanical Metallurgy Division, Indira Gandhi Centre for Atomic Research, Kalpakkam – 603 102, Tamil Nadu, India
M.D. Mathew: Mechanical Metallurgy Division, Indira Gandhi Centre for Atomic Research, Kalpakkam – 603 102, Tamil Nadu, India

1 Introduction

9Cr-1Mo ferritic steel is widely used for steam generator applications in fossil fired thermal and nuclear power generating industries. The steel is also an important candidate material for all the components such as tube, shell and thick section tubeplate of steam generators of sodium cooled fast reactors (SFRs). The selection of 9Cr-1Mo steel for steam generator application in SFRs is based on its low thermal expansion co-efficient, high resistance to stress corrosion cracking compared to austenitic steels and superior mechanical properties at elevated temperatures than the alternate 2.25Cr-1Mo steel [1, 2]. In addition to above, 9Cr-1Mo steel offers good combination of high creep strength and ductility, good weldability and microstructural stability over long exposure at elevated temperatures [1, 2]. The steel also offers nearly uniform microstructure over large section size due to its high hardenability [3]. Use of 9Cr-1Mo steel as a single structural material in steam generators of SFRs enhances the reliability of the components including critical tube to tubeplate welds. The steel has also emerged as an important candidate material for wrapper applications in future SFRs due to its high resistance to irradiation creep and void swelling compared to austenitic steels [4, 5]. 9Cr-1Mo steel displays three distinct temperature regimes for the variations of tensile strength, average work hardening rate and ductility with respect to temperature [6, 7]. At intermediate temperatures, the steel exhibits serrated flow, an important manifestation of dynamic strain ageing (DSA) accompanied with plateaus/peaks in flow stress and average work hardening rate, negative strain rate sensitivity of flow stress and ductility minima [6–8]. Comparative evaluation of elevated temperature tensile properties of normalised and tempered thin section plate and quenched and tempered thick section tubeplate forging of 9Cr-1Mo ferritic steel indicated consistently lower yield and ultimate tensile strength values accompanied with higher ductility of the forging due to the effects associated with coarseness of microstructure [9].

Tensile flow and work hardening behaviour attract continued scientific and technological interest in view of improving the appropriate conditions for material processing and ensuring safe performance during service. Among the several relationships [10–15] proposed to describe tensile flow and work hardening behaviour of metals and alloys, Voce relation [12, 14] has attracted more

attention in view of the sound interpretation provided by Kocks-Mecking (K-M) [16–19] through phenomenological approach by using dislocation density as a single structural parameter. The work hardening is controlled by the competition between storage and annihilation (rearrangement) of dislocations, which are assumed to superimpose in an additive manner. Accordingly, the linear decrease in instantaneous work hardening rate θ ($\theta = d\sigma/d\varepsilon_p$, where σ is true stress and ε_p is true plastic strain) with increasing stress in stage-III [16, 17] is expressed as

$$\theta = \theta_0\left(1-\frac{\sigma}{\sigma_S}\right) \quad (1)$$

where θ is work hardening rate at stress σ, θ_0 is initial work hardening rate and σ_S is saturation stress at high strains corresponding to condition where instantaneous work hardening rate is equal to zero, i.e. $\theta = 0$. It has been demonstrated that the tensile flow behaviour of both plate and tubeplate forging of 9Cr-1Mo steel is described most accurately by a combination of Ludwigson and Hollomon equations [20, 21]. Ludwigson equation describes stress-strain behaviour most appropriately at room and intermediate temperatures. At high temperatures, Ludwigson equation reduces to Hollomon equation. Alternately, Voce equation as a single relationship has been suggested to describe tensile flow behaviour adequately for the range of temperatures of interest for useful engineering applications [20, 21].

Following Kocks-Mecking approach [16, 17], tensile work hardening behaviour of 9Cr-1Mo steel in the two different product forms namely normalised and tempered plate material and thick section tubeplate forging in quenched and tempered condition has been investigated in terms of the variation of instantaneous work hardening rate (θ) with true stress (σ) in the temperature range 300–873 K. In view of significant influence of temperature on θ-σ, an attempt has been made to evolve a unified description of tensile work hardening behaviour in terms of the variations in θ with plastic strain rate ($\dot{\varepsilon}_p$) for both plate and tubeplate forging for the temperature range 300–873 K. The variations of θ with respect to $\dot{\varepsilon}_p$ exhibited an interesting correlation between θ and $\dot{\varepsilon}_p$ in terms of a single master curve for both plate and tubeplate forging for the range of temperatures investigated. The variations of θ have been also examined in terms of the reciprocal of plastic strain rate, i.e. $1/\dot{\varepsilon}_p$ for both plate and forging.

2 Experimental details

The chemical composition of 9Cr-1Mo steel in two different forms, i.e. plate of 20 mm thickness and tubeplate forging of 1000 mm diameter and 300 mm thickness used in this study is given in Table 1. Normalised and tempered (N + T) 20 mm plate was supplied by Creusot-Loire industries, France. The hot rolled plate was normalised at 1223 K for 15 min followed by air cooling and tempered at 1053 K for 2 h followed by air cooling. The hot forged tubeplate forging of 1000 mm diameter and 300 mm thickness in quenched and tempered (Q + T) condition was obtained from BRUCK, GmbH, Germany. Tubeplate forging was austenitised with controlled heating (heating time 8 h) to 1223 K and soaking at 1223 K for 5 h followed by quenching in water. Tempering treatment involved controlled heating (heating time 8 h) to 1023 K and soaking at 1023 K for 8 h followed by air cooling. Metallographic examinations were performed on N + T plate and Q + T tubeplate specimens prepared using standard metallographic techniques and by immersion etching in 1 g picric acid + 5 ml HCl + 100 ml ethyl alcohol. The microstructure of N + T plate consisted of fine tempered lath martensite and fine precipitates at the boundaries of prior austenite grains and martensite laths and in intralath matrix regions. Average prior austenite grain size measured by linear intercept method was ~25 μm for plate material. Tubeplate forging exhibited coarse tempered lath martensite and a few stringers of pro-eutectoid ferrite at prior austenite grain boundaries. Using point count method, pro-eutectoid ferrite was estimated as ~2% in the surface and along the thickness within 300 mm outer annulus of the forging. Tubeplate forging displayed coarse prior austenite grain size of 120 μm. In general, tubeplate forging displayed coarser austenite grain, martensite packets and lath martensite

Product form	Element (wt.%)							
	C	Cr	Mo	Si	Mn	S	P	Fe
20 mm plate	0.10	8.44	0.95	0.48	0.45	0.002	0.008	Balance
Tubeplate forging	0.10	9.27	1.05	0.75	0.63	0.001	0.02	Balance

Table 1: Chemical composition (wt.%) of plate and tubeplate of 9Cr-1Mo steel.

and coarse precipitates than those shown by plate material. The microstructures of both plate and tubeplate forging have been described in detail in Ref. [9].

Specimen blanks of 12 mm diameter and 60 mm length were machined with stress axis in rolling direction from plate material. For tubeplate forging, 12 mm diameter and 60 mm long specimen blanks were machined with stress axis in the thickness direction from the outer annulus of 300 mm width. Cylindrical button head tensile specimens with 4 mm gauge diameter and 26 mm gauge length were machined. Tensile tests were performed in air in a floor model Instron 1195 universal testing machine equipped with a three-zone temperature control furnace and a stepped-load suppression unit. Tests were performed on plate and tubeplate specimens over temperature range 300–873 K at a nominal strain rate of 1.26×10^{-3} s^{-1}. Test temperatures were controlled within ±2 K. Load-elongation curves were recorded using the Instron autographic recorder for all the tests. Use of suitable chart speed and stepped zero suppression gave strain and stress resolutions of 7.5×10^{-4} and 0.80 MPa, respectively.

3 Analysis of data

9Cr-1Mo steel in both the product forms, i.e. plate and tubeplate forging exhibited serrated (jerky) load-elongation curves at intermediate temperatures in the range 523–698 K. At room and high temperatures, smooth load-elongation curves were observed for both plate and tubeplate forging. Based on the definition and classification of serrations [22], an averaging scheme for measuring load values for different types of serrations observed for both plate and tubeplate forging has been adopted. For type A serrations showing an abrupt rise in the loads followed by discontinuous drops to or below the general level of load-elongation curves, general levels of load values were considered. For type B serrations that oscillate about the general level of load values, mean load values were taken. Envelope load values were considered for type C serrations characterised by load drops always below the general level of load-elongation curves. The averaging scheme of load-elongations values for different types of serrations for plate and tubeplate forging are presented in Ref. [20, 21]. The true stress (σ)-true plastic strain (ε_p) data were evaluated using a computer program from the digitized load-elongation data up to the maximum load values. Since, no strain gauge was employed, the cross head displacement was taken as the specimen extension. The linear elastic portion of load-elongation data contributed by the specimen, machine frame and load-train assembly was subtracted from the total elongation by appropriately using the slope of the initial linear portion for the calculation of plastic strain. Stress and plastic strain data were used to determine true stress and true plastic strain. Instantaneous work hardening rate (θ) and plastic strain rate ($\dot{\varepsilon}_p$) were obtained from the numerical differentiation of σ-ε_p and ε_p-time (t) data, respectively.

4 Results and discussion

4.1 Influence of temperature on θ vs. σ behaviour for plate and tubeplate forging

At all temperatures, θ vs. σ plots exhibited an initial rapid decrease in θ at low stresses followed by a gradual decrease in θ with σ at high stresses for both plate and tubeplate forging. The variations in θ as a function of σ for both plate and tubeplate forging at 300, 573 and 873 K representing room, intermediate and high temperatures, respectively, are shown in Figure 1 as an example. The variations of respective true plastic strain rate ($\dot{\varepsilon}_p$) with true stress are also superimposed in Figure 1. The initial rapid decrease in θ is designated as transient stage (or TS) and the gradual decrease in θ represents typical stage-III work hardening governed by Kocks-Mecking approach. The distinction between transient stage and stage-III is shown at room and intermediate temperatures in Figs. 1a and 1b, respectively for plate material. This distinction is not shown for 873 K in absence of a sharp division between the two stages at high temperatures. At all temperatures, θ-σ for tubeplate forging lies at lower stresses, i.e. more towards origin than those for plate material. Accordingly, tubeplate forging exhibited lower stresses for the occurrence of transient stage and stage-III and for the onset of stage-III than those for plate material. Further, tubeplate forging exhibited consistently lower rates of decrease in work hardening rates in θ-σ than those observed for plate material. This is discernable from the low values of slopes of θ vs. σ plots in stage-III for tubeplate forging. The variations of instantaneous work hardening rate, θ with stress for both plate and tubeplate forging displayed a general shift in θ-σ towards low stresses with increase in temperature. θ-σ for both plate and tubeplate forging exhibited three temperature regimes as a shift to low stresses with increase in temperature from 300 to 523 K followed by an insignificant shift at intermediate temperatures and a rapid shift at high temperatures. At intermediate temperatures, θ-σ data fall in a narrow band and no significant

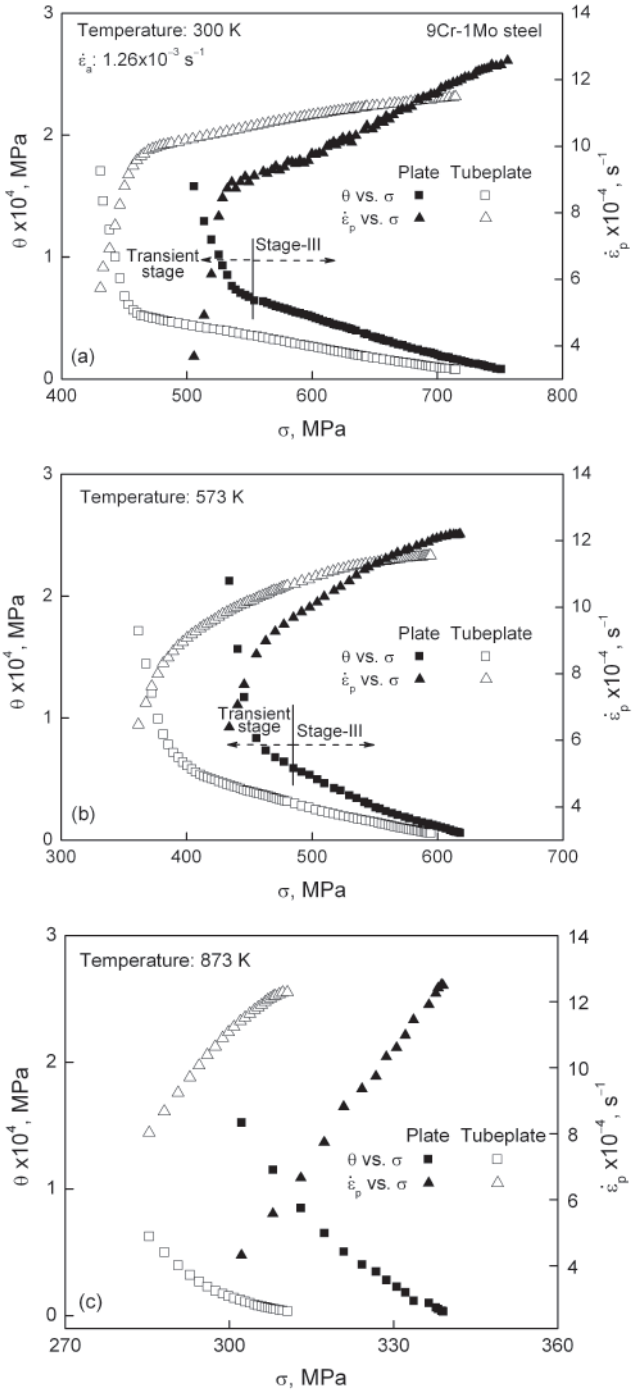

Fig. 1: Variations of work hardening rate (θ) and true plastic strain rate ($\dot{\varepsilon}_p$) as a function of true stress (σ) at (a) 300, (b) 573 and (c) 873 K for plate and tubeplate forging of 9Cr-1Mo steel.

variations in θ-σ with respect to temperature are observed. At high temperatures beyond 723 K, a rapid shift in θ-σ towards origin with increasing temperature is observed. The variations of instantaneous work hardening rate, θ with stress for tubeplate forging is shown in Figure 2 as an example. θ = σ line is also shown as broken line in Figure 2.

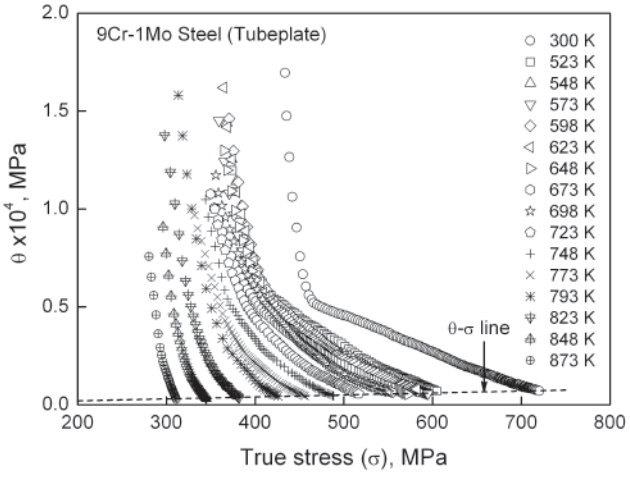

Fig. 2: Variations of work hardening rate (θ) as a function of true stress (σ) at various temperatures for 9Cr-1Mo steel tubeplate forging.

Two-stage work hardening behaviour observed in the variations of θ with σ for 9Cr-1Mo steel plate and tubeplate forging is consistent with those observed for 9% Cr steel [23, 24]. 9Cr-1Mo steel having high stacking fault energy exhibited transient stage at low stresses only. Thereafter, the recovery dominant stage-III is manifested as a gradual decrease in θ with σ. The influence of temperature on θ-σ behaviour in both plate and tubeplate forging showing distinct three temperature regimes is also consistent with earlier observations on 9% Cr steels [24]. The occurrence of dynamic strain ageing at intermediate temperatures in the steel is reflected in the grouping of θ-σ data with respect to temperature in a narrow band (Figure 2). Measurement of activation energy from the strain rate and temperature dependence of critical strain for the onset of serrated flow indicated that diffusion of interstitial solute such as carbon is responsible of dynamic strain ageing in 9Cr-1Mo steel [6–8]. At intermediate temperatures, DSA causes an increased rate of dislocation multiplication and delay in recovery of dislocation structure due to reduced propensity to cross-slip [25–29]. Reduced propensity to cross-slip results from pinning of dislocations by diffusing solutes and thereby preventing screw dislocation to cross-slip due to its reduced mobility. Contrary to this, rapid shift in θ-σ plots to lower stresses with increasing temperature beyond 723 K indicate dominance of recovery processes due to early cross-slip and climb of dislocations at high temperatures. It has been shown that dominance of recovery at high temperatures results in the formation of regular subboundaries, and subgrains, decrease in dislocation density and increase in subgrain size with increase in temperature [26, 28].

At all temperatures, the occurrence of θ-σ for tubeplate forging at comparatively lower stresses than for plate material can be ascribed to the lower strength of the forging (Figure 1). Based on the comparative evaluation of tensile properties of plate and tubeplate forging, it has been suggested that the inferior tensile strength of tubeplate forging results from coarseness of microstructure in terms of coarse prior austenitic grain and martensite packet and lath martensite size, relatively low dislocation density and coarse precipitates [9]. Coarse austenitic grain size of ~120 μm originates from relatively high hot forging temperature and extended heat treatment of slow heating to austenitising temperature and soaking for 5 h. Slow cooling rate due to large section size results in coarse martensite packets and lath martensite. Extended tempering treatment of slow heating to tempering temperature and soaking for 8 h leads to coarser precipitates and higher inter-barrier distance for dislocation motion in the forging [9].

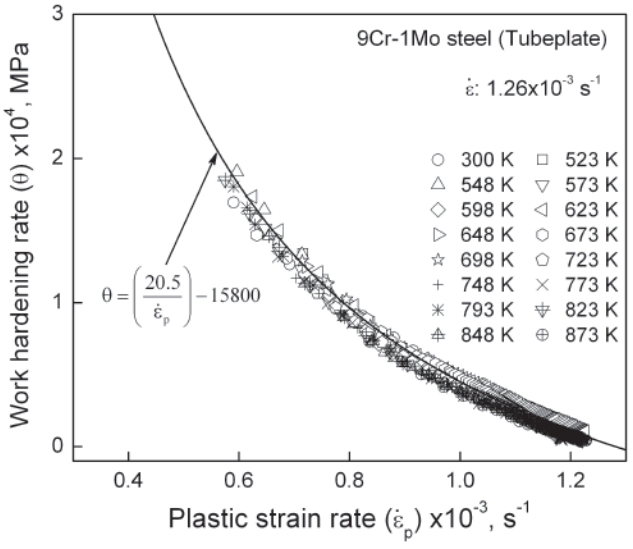

Fig. 3: Variations of work hardening rate (θ) as a function of true plastic strain rate ($\dot{\varepsilon}_p$) at different temperatures for 9Cr-1Mo steel tubeplate forging. Solid line is according to Eq. (2).

4.2 Influence of temperature on θ vs. $\dot{\varepsilon}_p$ behaviour for plate and tubeplate forging

In order to understand the large influence of temperature and different initial microstructures (due to different processing routes and section size) on tensile work hardening behaviour of 9Cr-1Mo steel (Figs. 1 and 2), the variations of instantaneous work hardening rate have been examined with respect to plastic strain rate at all temperatures in both plate and tubeplate forging. The variations of plastic strain rate and work hardening rate as a function of stress for both plate and tubeplate forging indicated that $\dot{\varepsilon}_p$ varies with σ in opposite manner to those observed for θ vs. σ (Figure 1). $\dot{\varepsilon}_p$ increases rapidly with similar rapid decrease in θ in the transient stage followed by gradual increase in $\dot{\varepsilon}_p$ in stage-III. The onset of stage-III is observed when $\dot{\varepsilon}_p$ reaches ~70% of the imposed strain rate. Beyond this, a gradual increase in $\dot{\varepsilon}_p$ close to imposed strain rate is obtained at the onset of necking. Figure 3 shows the interrelationship between θ with $\dot{\varepsilon}_p$ in the plots of θ vs. $\dot{\varepsilon}_p$ for tubeplate forging in the temperature range 300–873 K. The large influence of temperature observed for θ vs. σ is absorbed into a master curve interrelating θ and $\dot{\varepsilon}_p$, independent of temperature. It can be also seen that the distinct two-stage work hardening behaviour in terms of θ vs. σ and $\dot{\varepsilon}_p$ vs. σ is not visible in the curvilinear plots of θ vs. $\dot{\varepsilon}_p$ in Figure 3. An inverse correlation between θ and $\dot{\varepsilon}_p$ independent of temperature has been obtained as linear plots of θ vs. reciprocal of plastic strain rate, i.e. $1/\dot{\varepsilon}_p$

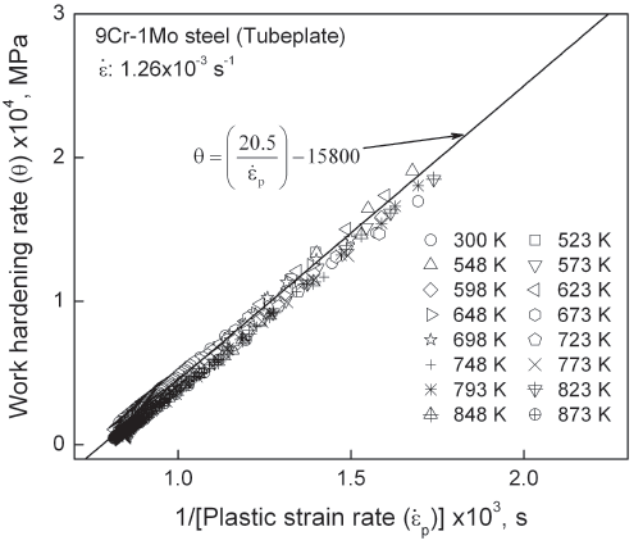

Fig. 4: Variations of work hardening rate (θ) as a function of reciprocal of true plastic strain rate ($1/\dot{\varepsilon}_p$) at different temperatures for 9Cr-1Mo steel tubeplate forging. Solid line is according to Eq. (2).

(Figure 4). A master curve obtained from the least square optimisation obeying θ-$\dot{\varepsilon}_p$ data for 300–873 K is superimposed as solid lines in Figs. 3 and 4. The θ-$\dot{\varepsilon}_p$ relation for tubeplate forging is obtained as

$$\theta = \left(\frac{20.5}{\dot{\varepsilon}_p}\right) - 15800. \quad (2)$$

The analysis of σ–ε_p data in terms of the rate of change of true stress (dσ/dt) with respect to true plastic strain rate ($\dot{\varepsilon}_p = d\varepsilon_p/dt$) resulted in a linear master plot of dσ/dt vs. $\dot{\varepsilon}_p$

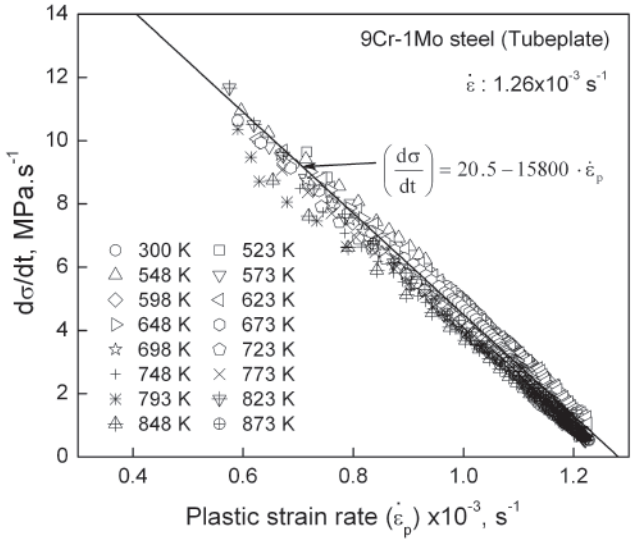

Fig. 5: Variations of true stress rate (dσ/dt) as a function of true plastic strain rate ($\dot{\varepsilon}_p = d\varepsilon_p/dt$) at different temperatures for 9Cr-1Mo steel tubeplate forging. Solid line is according to Eq. (3).

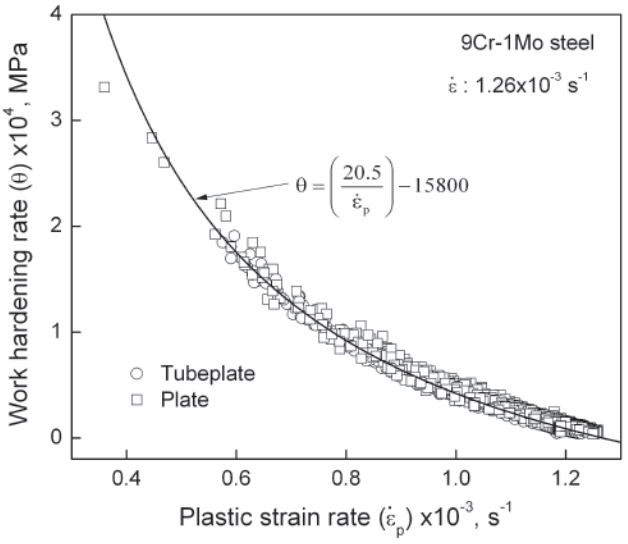

Fig. 6: Variations of work hardening rate (θ) as a function of true plastic strain rate ($\dot{\varepsilon}_p$) in the temperature range 300–873 K for plate and tubeplate forging of 9Cr-1Mo steel. Solid line is according to Eq. (2).

for temperature range 300–873 K (Figure 5). The master curve interrelating dσ/dt vs. $\dot{\varepsilon}_p$ obeying Eq. (3) as

$$\left(\frac{d\sigma}{dt}\right) = 20.5 - 15800 \cdot \dot{\varepsilon}_p, \qquad (3)$$

has been superimposed in Figure 5. The values of dσ/dt were estimated from the numerical differentiation of σ-t data. The linear variations of dσ/dt vs. $\dot{\varepsilon}_p$ suggest that the rate of change of true stress is directly proportional to the respective true plastic strain rate during the course of deformation in 9Cr-1Mo steel.

Normalised and tempered plate material also exhibited similar unified work hardening behaviour in terms of θ-$\dot{\varepsilon}_p$, θ-1/$\dot{\varepsilon}_p$ and dσ/dt-$\dot{\varepsilon}_p$ for the temperature range 300–873 K. In order to investigate the influence of microstructure on the variations of θ with $\dot{\varepsilon}_p$, θ-$\dot{\varepsilon}_p$ data in two different product forms, i.e. plate and tubeplate forging have been compared in Figure 6. Symbols represent θ-$\dot{\varepsilon}_p$ data for plate and tubeplate forging in the temperature range 300–873 K and the master work hardening curve obeying Eq. 2 is shown as solid line in Figure 6. It can seen that the large difference in θ-σ between plate and tubeplate forging observed in the temperature range 300–873 K (Figure 1) is not visible in plots of θ vs. $\dot{\varepsilon}_p$ for plate and tubeplate forging (Figure 6). Like in Figure 4, an inverse correlation between θ and $\dot{\varepsilon}_p$ independent of temperature has been also obtained for both plate and tubeplate forging for the temperature range 300–873 K (Figure 7). The master work hardening curve representing both plate and tubeplate forging following Eq. 2 for the temperature

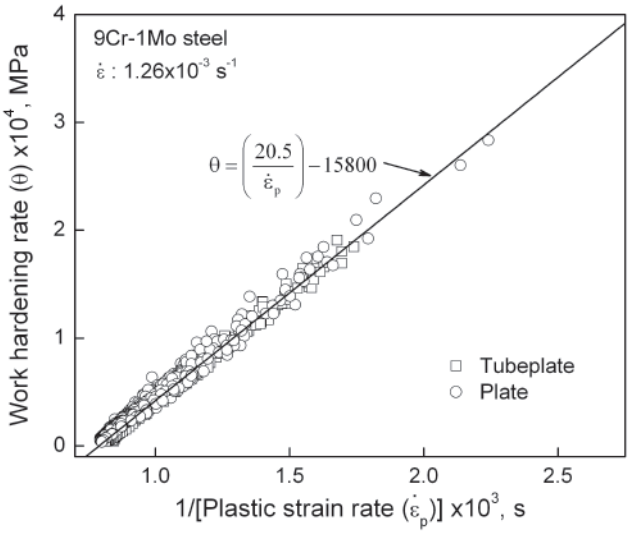

Fig. 7: Variations of work hardening rate (θ) as a function of reciprocal of true plastic strain rate (1/$\dot{\varepsilon}_p$) in the temperature range 300–873 K for plate and tubeplate forging of 9Cr-1Mo steel. Solid line is according to Eq. (2).

range 300–873 K is shown as solid line in Figure 7. As a consequence to an inverse correlation between θ and $\dot{\varepsilon}_p$, proportionality between rate of change of true stress dσ/dt and true plastic strain $\dot{\varepsilon}_p$ for both plate and tubeplate forging independent of microstructure and temperature is shown in Figure 8. The observed inter-relationships between θ and $\dot{\varepsilon}_p$ (Figs. 6 and 7) and between dσ/dt and $\dot{\varepsilon}_p$ (Figure 8) for 9Cr-1Mo steel is interesting. The distinct two-stage working hardening, large influence of temperature

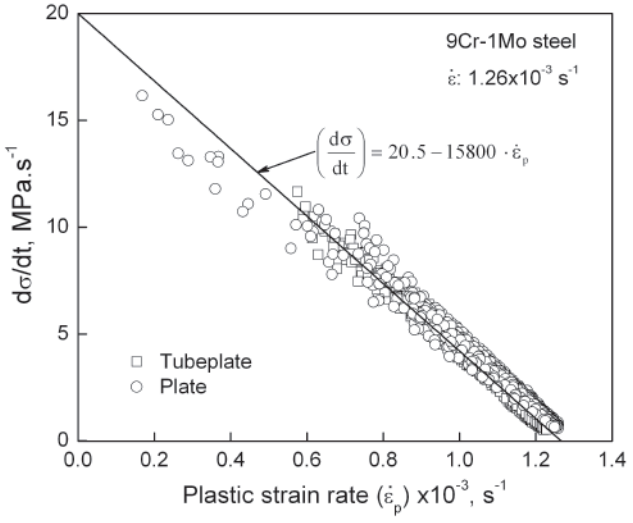

Fig. 8: Variations of true stress rate ($d\sigma/dt$) as a function of true plastic strain rate ($\dot{\varepsilon}_p = d\varepsilon_p/dt$) in the temperature range 300–873 K for plate and tubeplate forging of 9Cr-1Mo steel. Solid line is according to Eq. (3).

and microstructure on θ-σ (Figs. 1 and 2) are absorbed into curvilinear θ-$\dot{\varepsilon}_p$ (Figure 6) and linear θ-$1/\dot{\varepsilon}_p$ (Figure 7) and $d\sigma/dt$-$\dot{\varepsilon}_p$ (Figure 8) master curves in spite of the differences in dominating deformation mechanisms at room, intermediate and high temperatures. The observed master work hardening curve for θ vs. $\dot{\varepsilon}_p$ or θ vs. $1/\dot{\varepsilon}_p$ indicate that for a constant value of θ, a constant value of plastic strain rate is generated irrespective of difference in the dominating deformation mechanisms in the temperature range 300–873 K for different initial microstructures. The generation of plastic strain rate is constrained by the applied strain rate. For the two different initial microstructures, the evolution of plastic strain with stress is governed by the ability of the material to deform under imposed modes of deformation at room, intermediate and high temperatures in such a way that for a fixed value of θ, a fixed value of $\dot{\varepsilon}_p$ is generated. This universal evolution of plastic strain and increase in flow stress leads to unified work hardening in terms of θ vs. $\dot{\varepsilon}_p$.

5 Conclusions

At all temperatures, the variations of instantaneous work hardening rate (θ) with true stress (σ) exhibited two-stage behaviour characterised by a rapid decrease in θ at low stresses (transient stage) followed by a gradual decrease at high stresses (stage-III) for both plate and tubeplate forging in 9Cr-1Mo steel. The influence of temperature is reflected in a shift in θ-σ plots to low stresses depicting three temperature regimes of room, intermediate and high temperatures. The influence of initial microstructure is also reflected in a shift in θ-σ plots to low stresses due to inferior strength of the forging in the temperature range 300–873 K. An interesting correlation between θ and plastic strain rate is obtained as a single master curve for the temperature range 300–873 K and for different product forms, i.e. plate and tubeplate forging. The variations of θ with reciprocal of $\dot{\varepsilon}_p$ provided linear master curve independent of temperature and initial microstructure. As a consequence, the rate of change of true stress is linearly related with the true plastic strain rate independent of temperature and initial microstructure.

Received: July 17, 2012. Accepted: October 19, 2012.

References

[1] B.J. Cane and R.S. Fidler, *Ferritic Steels for Fast Reactor Steam Generators*, S.F. Pugh and E.A. Little (Eds.), 1977, pp. 193–199, British Nuclear Energy Society, London.
[2] V.K. Sikka, *Ferritic Alloys for Use in Nuclear Energy Technologies*, J.W. Davies and D.J. Michael (Eds.), 1984, pp. 317–327, TMS-AIME, Warrendale, PA.
[3] S.J. Sanderson, *Ferritic Steels for High Temperature Applications*, Ashok K. Khare (Ed.), 1981, pp. 85–99, ASM, Metals Park, OH.
[4] A. Alamo, J.L. Bertin, V.K. Shamardin and P. Wident, *J Nucl Mater*, **367–370**, 54 (2007).
[5] K.J. Harrelson, S.H. Rou and R.C. Wilcox, *J Nucl Mater*, **141–143**, 508 (1986).
[6] B.K. Choudhary, K.B.S. Rao, S.L. Mannan and B.P. Kashyap, *J Nucl Mater*, **273**, 315 (1999).
[7] B.K. Choudhary, V.S. Srinivasan and M.D. Mathew, *Mater High Temp*, **28**, 155 (2011).
[8] B.K. Choudhary, K.B.S. Rao, S.L. Mannan and B.P. Kashyap, *Mater Sci Technol*, **15**, 791 (1999).
[9] B.K. Choudhary, *High Temp Mater Proc*, **31**, 27 (2012).
[10] P. Ludwik, *Elements der Technologischen Mechanik*, 1909, p. 32. Verlag Von Julius Springer, Leipzig.
[11] J.H. Hollomon, *Trans AIME*, **162**, 268 (1945).
[12] E. Voce, *J Inst Met*, **74**, 537 (1948).
[13] H.W. Swift, *J Mech Phys Solids*, **1**, 1 (1952).
[14] E. Voce, *Metallurgia*, **51**, 219 (1955).
[15] D.C. Ludwigson, *Metall Trans*, **2**, 2825 (1971).
[16] U.F. Kocks, *J Eng Mater Technol*, **98**, 76 (1976).
[17] H. Mecking and U.F. Kocks, *Acta Metall*, **29**, 1865 (1981).
[18] Y. Estrin and H. Mecking, *Acta Metall*, **32**, 57 (1984).
[19] U.F. Kocks and H. Mecking, *Prog Mater Sci*, **48**, 171 (2003).
[20] D.P. Rao Palaparti, B.K. Choudhary, E. Isaac Samuel, V.S. Srinivasan and M.D. Mathew, *Mater Sci Eng* A, **538**, 110 (2012).
[21] D.P. Rao Palaparti, B.K. Choudhary and T. Jayakumar, *Trans Indian Inst Met*, (2012), DOI: 10.1007/s12666-012-0146-5.
[22] E. Pink and A. Grinberg, *Mater Sci Eng*, **51**, 1 (1981).
[23] R. Bonade and P. Spatig, *Mater Sci Eng* A, **400–401**, 234 (2005).

[24] J. Christopher, B.K. Choudhary, E. Isaac Samuel, V.S. Srinivasan and M.D. Mathew, *Mater Sci Eng* A, **528**, 6589 (2011).
[25] D.J. Dingley and D. McLean, *Acta Metall*, **15**, 885 (1967).
[26] D.J. Michel, J. Moteff and A.J. Lovell, *Acta Metall*, **21**, 1269 (1973).
[27] J.W. Edington and R.E. Smallman, *Acta Metall*, **12**, 1313 (1964).
[28] B.P. Kashyap, K. McTaggart and K. Tangri, *Philos Mag*, **57**, 97 (1988).
[29] S. Okamato, D.K. Matlock and G. Krauss, *Scripta Metall*, **25**, 39 (1991).